Deformed harmonic oscillators for metal clusters: Analytic properties and supershells

Dennis Bonatsos,[1,*] D. Lenis,[1] P. P. Raychev,[2,†] and P. A. Terziev[2,‡]
[1]*Institute of Nuclear Physics, NCSR "Demokritos," GR-15310 Aghia Paraskevi, Attiki, Greece*
[2]*Institute for Nuclear Research and Nuclear Energy, Bulgarian Academy of Sciences, 72 Tzarigrad Road, BG-1784 Sofia, Bulgaria*
(Received 30 July 2001; published 14 February 2002)

The analytic properties of Nilsson's modified oscillator, which was first introduced in nuclear structure, and of the recently introduced, based on quantum algebraic techniques, three-dimensional q-deformed harmonic oscillator (3D q-HO) with $u_q(3)\supset so_q(3)$ symmetry, which is known to reproduce correctly in terms of only one parameter the magic numbers of alkali clusters up to 1500 (the expected limit of validity for theories based on the filling of electronic shells), are considered. Exact expressions for the total energy of closed shells are determined and compared among them. Furthermore, the systematics of the appearance of supershells in the spectra of the two oscillators is considered, showing that the 3D q-HO correctly predicts the first supershell closure in alkali clusters without use of any extra parameter.

DOI: 10.1103/PhysRevA.65.033203 PACS number(s): 36.40.Cg, 03.65.Fd

I. INTRODUCTION

Supershells, which are seen as beats of the deviation of the total energy of many-particle systems from the function describing its average behavior vs the number of particles N, are known to be a general property of the spectrum of potentials having sharp edges [1]. Supershells in metal clusters were first studied by Nishioka, Hansen, and Mottelson [2] in terms of phenomenological mean-field potentials.

On the other hand, using recently developed quantum algebraic techniques [3], it has been shown [4] that the magic numbers appearing in alkali clusters can be successfully reproduced up to 1500 (which is the expected limit of validity of theories based on the filling of electronic shells [5]) by the three-dimensional q-deformed harmonic oscillator (3D q-HO), which possesses the $u_q(3)\supset so_q(3)$ symmetry [6]. Furthermore, the magic numbers appearing in several divalent (Zn, Cd) and trivalent (Al, In) metal clusters have been satisfactorily reproduced [4] by the same model in terms of only one free parameter, the deformation parameter τ (with $q=e^{\tau}$, where τ is a real number). It is therefore of interest to examine if the 3D q-HO can predict supershells and which these predictions are. It should be noticed that the calculation of supershells in the framework of the 3D q-HO will be parameter-free, since the single parameter of the model has been fixed in reproducing the magic numbers for each kind of cluster [4].

In addition to the 3D q-HO, Nilsson's modified oscillator (MO) [7,8], which has first been used in describing the structure of atomic nuclei, has also been employed earlier in describing atomic clusters [9] (after dropping the spin-orbit interaction, which plays an essential role in nuclear structure but is absent in the case of atomic clusters). It is therefore of interest to study the possible appearance of supershells in the framework of this model as well.

For the determination of supershells, the method of Ref. [2] can be employed. Before doing so, one has however to examine the analytic properties of the spectra of the two oscillators in order to be able to apply meaningful truncation schemes. Furthermore, the average behavior of the total energy of a system of many particles (an atomic cluster in the present case) as a function of the particle number N should be determined, since it is needed in the procedure of the study of supershells. As a result, these tasks will be carried out for both models, before any attempt at the determination of supershells is made.

Supershells have been predicted earlier by Balian and Bloch [10] in the study of electrons moving in a spherical cavity, which by analogy can be used for the valence electrons in a metal cluster. The comparison of the stringent predictions of the theory of Balian and Bloch for various characteristics of the supershells [1] to the results of the present models turns out to be a fruitful testing procedure.

In Sec. II the analytic properties of Nilsson's modified oscillator will be considered, while the corresponding properties of the 3D q-HO will be studied in Sec. III. In Sec. IV supershells in Nilsson's modified oscillator will be studied, while supershells in the framework of the 3D q-HO will be considered in Sec. V. Finally in Sec. VI a discussion of the present results and plans for further work will be given.

II. NILSSON'S MODIFIED OSCILLATOR

The potential of the MO introduced in nuclear physics by Nilsson [7,8] (with the spin-orbit term omitted) is

$$V=\frac{1}{2}\hbar\omega\rho^2-\hbar\omega\mu'(\mathbf{L}^2-\langle\mathbf{L}^2\rangle_n),\quad \rho=r\sqrt{\frac{M\omega}{\hbar}},\quad (1)$$

where

$$\langle\mathbf{L}^2\rangle_n=\frac{n(n+3)}{2}.\quad (2)$$

The effect of the $\mathbf{L}^2$ term is to flatten the bottom of the potential. In addition it causes an overall compression of the

*Email address: bonat@mail.demokritos.gr
†Email address: raychev@inrne.bas.bg
‡Email address: terziev@inrne.bas.bg

spectrum, which is avoided through the addition of the $\langle \mathbf{L}^2 \rangle_n$ term, which will be further discussed later.

The energy eigenvalues of Nilsson's modified harmonic oscillator are [7,8]

$$E_{nl} = \hbar\omega(n+\tfrac{3}{2}) - \hbar\omega\mu'[l(l+1) - \tfrac{1}{2}n(n+3)], \quad (3)$$

where n is the number of vibrational quanta and l is the eigenvalue of the angular momentum, obtaining the values $l = n, n-2, \ldots, 0$ or 1 (depending on n being even or odd, respectively).

The number of states having energy $(n+3/2)\hbar\omega$ in the case of even n is

$$n_1 = \sum_{l=0, l=\text{even}}^{n} (2l+1) = \frac{(n+1)(n+2)}{2}, \quad (4)$$

where only the even values of l are included in the summation and the sum

$$\sum_{x=1}^{n} x = \frac{n(n+1)}{2} \quad (5)$$

has been used. The same result is obtained for odd n, in which case only the odd values of l are included in the summation. Taking into account the spin of the particles, the number of states having energy $(n+3/2)\hbar\omega$ is

$$n_2 = (n+1)(n+2). \quad (6)$$

The sum of the eigenvalues of $\mathbf{L}^2$ within each shell in the case of even n is

$$L_1 = \sum_{l=0, l=\text{even}}^{n} l(l+1)(2l+1) = \frac{n(n+1)(n+2)(n+3)}{4}, \quad (7)$$

where only the even values of l have been included in the summation and, in addition to Eq. (5), the sums

$$\sum_{x=1}^{n} x^2 = \frac{n(n+1)(2n+1)}{6} \quad (8)$$

and

$$\sum_{x=1}^{n} x^3 = \frac{n^2(n+1)^2}{4} \quad (9)$$

have been taken into account. The same result is obtained for n being odd. Taking the spin of the particles into account, one has

$$L_2 = 2L_1 = \frac{n(n+1)(n+2)(n+3)}{2}. \quad (10)$$

Thus the average per particle of the square of the angular momentum within each shell is

$$\langle \mathbf{L}^2 \rangle_n = \frac{L_1}{n_1} = \frac{L_2}{n_2} = \frac{n(n+3)}{2}, \quad (11)$$

a result that has already been used in Eqs. (1) and (3), in order to keep the ''center of mass'' of each shell constant, i.e., to counterbalance the overall compression of the spectrum caused by the $\mathbf{L}^2$ term alone.

The total number of particles that can be accommodated in the levels of the shells up to the nth shell included is

$$N = \sum_{x=0}^{n} (x+1)(x+2) = \frac{(n+1)(n+2)(n+3)}{3}, \quad (12)$$

where the spin of the particles has been taken into account and Eqs. (5), (6), and (8) have been used. It should be remembered throughout the present work that N stands for the total number of particles, while n stands for the number of vibrational quanta.

The contribution of the first term of Eq. (3) to the total energy of the particles up to the nth shell included (and taking the spin of the particles into account) is

$$E(n) = \hbar\omega \sum_{x=0}^{n} \left(x + \frac{3}{2}\right)(x+1)(x+2) = \hbar\omega \frac{(n+1)(n+2)^2(n+3)}{4}, \quad (13)$$

where Eq. (6) is used for the degeneracy within each shell and Eqs. (5), (8), and (9) have been used for performing the summations. For later use we notice that omitting the ground-state energy contribution in a similar manner one finds

$$E'(n) = \hbar\omega \sum_{x=0}^{n} x(x+1)(x+2) = \hbar\omega \frac{n(n+1)(n+2)(n+3)}{4}, \quad (14)$$

while an n^2 perturbation in the energy would have given an additional term

$$E_2(n) = \hbar\omega \sum_{x=0}^{n} x^2(x+1)(x+2) = \hbar\omega \frac{n(n+1)(n+2)(n+3)(4n+1)}{20}, \quad (15)$$

where the sum

$$\sum_{x=1}^{n} x^4 = \frac{n(n+1)(2n+1)(3n^2+3n-1)}{30} \quad (16)$$

has been used in addition to Eqs. (5), (6), (8), and (9).

The contribution of the second term of Eq. (3) to the total energy of the particles up to the nth shell included is found by using Eq. (10),

$$E_3(n) = -\hbar\omega\mu' \sum_{x=0}^{n} \frac{x(x+1)(x+2)(x+3)}{2}, \quad (17)$$

while the contribution of the third term of Eq. (3) will be

$$E_4(n) = +\frac{1}{2}\hbar\omega\mu' \sum_{x=0}^{n} x(x+3)(x+1)(x+2), \quad (18)$$

where use of Eq. (6) has been made. We remark that $E_3(n)$ and $E_4(n)$ cancel. Thus we conclude that in Nilsson's MO only the first term of Eq. (3) contributes to the total energy of the particles up to the nth shell included.

The average energy per particle (up the nth shell included) is then found using Eqs. (12) and (13) to be

$$\langle E \rangle = \frac{E(n)}{N} = \hbar\omega\left(\frac{3}{4}n + \frac{3}{2}\right), \quad (19)$$

i.e., the average energy per particle is increasing linearly with the shell number, which is the number of vibrational quanta, as is expected for a harmonic oscillator, since the angular momentum terms make no contribution, as we have already seen. The same result is obtained from Eq. (14),

$$\langle E' \rangle = \frac{E'(n)}{N} = \hbar\omega\frac{3}{4}n, \quad (20)$$

where the 3/2 term has been omitted already in Eq. (14), while a n^2 perturbation in energy, as seen from Eqs. (12) and (15), would have given an extra term

$$\langle E_2(n) \rangle = \frac{E_2(N)}{N} = \hbar\omega\frac{3}{20}n(4n+1), \quad (21)$$

which naturally contains a n^2 term.

The lower part of the spectrum of Nilsson's modified oscillator, calculated from Eq. (3), is shown in Fig. 1(a) as a function of the parameter μ', together with the magic numbers appearing at different parameter values. The following observations can be made.

(a) The magic numbers at the left end of the figure are those of the three-dimensional isotropic harmonic oscillator.

(b) The magic numbers appearing around $\mu' = 0.04$ are in agreement with the magic numbers appearing in alkali clusters, up to 138 (see Ref. [4] for more details). The agreement is destroyed beyond this point.

(c) Around the parameter value $\mu' = 0.02$ the magic numbers up to 138 are a mixture of magic numbers of the three-dimensional isotropic harmonic oscillator and magic numbers appearing around $\mu = 0.04$ (magic numbers of alkali clusters).

(d) Equation (3) can be rewritten as

$$E_{nl} = \frac{3}{2}\hbar\omega + \hbar\omega n\left(1 + \frac{3\mu'}{2}\right) + \hbar\omega n^2\frac{\mu'}{2} - \hbar\omega\mu' l(l+1), \quad (22)$$

which clearly shows that in the case of $\mu' > 0$ the levels within each oscillator shell (characterized by a given value of n) are ordered according to the value of l, with the levels with higher values of l lying lower in energy, because of the last term in Eq. (22). This is indeed the case in Fig. 1(a), although the levels have not been labeled by the quantum numbers n,l because of lack of space.

(e) The level with $l = n$, in particular, lies lowest in energy within each shell and, in general, its energy is decreasing with increasing μ', since in this case Eq. (3) takes the form

$$E_{nn} = \frac{3}{2}\hbar\omega + \hbar\omega n\left(1 + \frac{\mu'}{2}\right) - \hbar\omega n^2\frac{\mu'}{2}, \quad (23)$$

its derivative with respect to μ' being

$$\frac{dE_{nn}}{d\mu'} = \hbar\omega\frac{1}{2}n(1-n), \quad (24)$$

which is indeed negative for $n > 1$. Indeed the levels that lie lowest within each oscillator shell in Fig. 1(a) are the levels with $l = n$, which also show negative slope with increasing μ'.

(f) The fact that the n^2 term in Eq. (23) appears with a negative sign (for $\mu' > 0$) can cause difficulties if one tries to describe a system with a large number of particles in terms of this oscillator. The derivative of E_{nn} with respect to n,

$$\frac{dE_{nn}}{dn} = \hbar\omega\left(1 + \frac{\mu'}{2} - \mu' n\right), \quad (25)$$

remains positive for

$$n < \frac{1}{\mu'} + \frac{1}{2}. \quad (26)$$

Beyond this value of n the derivative is negative, meaning that levels with higher values of n will lie lower in energy, making it difficult to define a cutoff for the number of shells taken into account. For example, if $\mu' = 0.04$ (a value that has been found [9] relevant to the description of metal clusters), the derivative remains positive if $n < 25.5$. It is then clear that a reasonable truncation of the spectrum is possible only if the number of shells to be taken into account is less than 26 (taking the $n = 0$ shell into account), otherwise no truncation is possible. This drawback of Nilsson's MO does not have any consequences in the case of nuclear structure, where the model has been first introduced, because of the small number of particles involved there [for which including the shells up to $n = 8$, shown in Fig. 1(a), suffices], but it can cause difficulties if one tries to employ this model for the determination of supershells in metal clusters, as we shall see later in Sec. IV.

(g) As an extension of (f), one sees from Eq. (23) that E_{nn} remains positive if $n < 2/\mu' + 1$. Thus, in the case of $\mu' = 0.04$ one should have $n < 51$, otherwise energies lower than the ground-state energy will occur.

III. THE THREE-DIMENSIONAL q-DEFORMED HARMONIC OSCILLATOR

The space of the three-dimensional q-deformed harmonic oscillator consists of the completely symmetric irreducible representations of the quantum algebra $u_q(3)$. In this space a

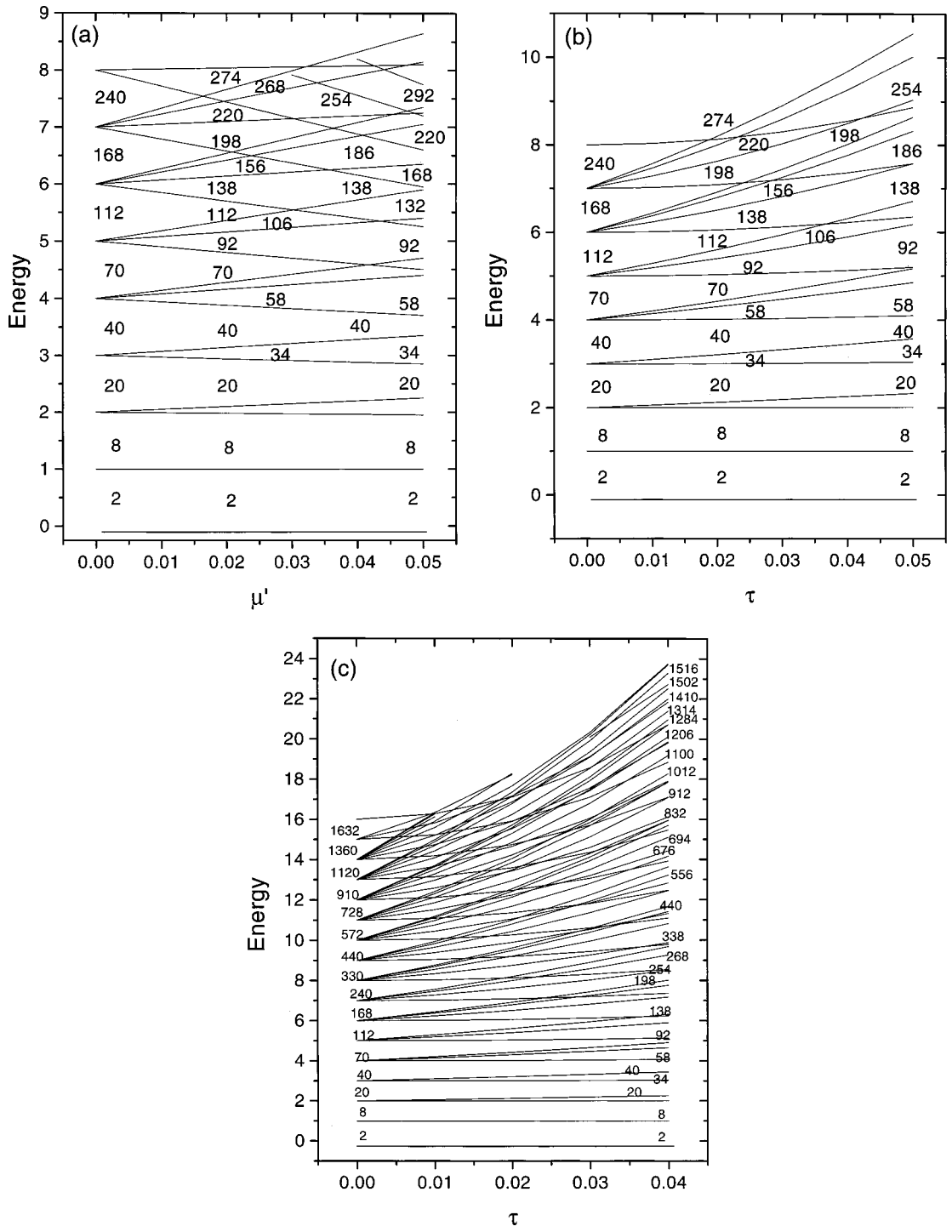

FIG. 1. (a) Energy spectrum of Nilsson's modified oscillator [in units of $\hbar\omega$, see Eq. (3)] as a function of the (dimensionless) model parameter μ'. Magic numbers are shown at the main gaps. (b) Energy spectrum of the 3D q-deformed harmonic oscillator [in units of $\hbar\omega_0$, see Eq. (29)] as a function of the (dimensionless) model parameter τ (with $q=e^{\tau}$, where τ is real). (c) Same as (b), but extended to higher energy levels.

deformed angular momentum algebra, $\mathrm{so}_q(3)$, can be defined [6]. The Hamiltonian of the three-dimensional q-deformed harmonic oscillator is defined so that it satisfies the following requirements.

(a) It is an $\mathrm{so}_q(3)$ scalar, i.e., the energy is simultaneously measurable with the q-deformed angular momentum related to the algebra $\mathrm{so}_q(3)$ and its z projection.

(b) It conserves the number of bosons, in terms of which the quantum algebras $\mathrm{u}_q(3)$ and $\mathrm{so}_q(3)$ are realized.

(c) In the limit $q\rightarrow 1$ it is in agreement with the Hamiltonian of the usual three-dimensional harmonic oscillator.

It has been proved [6] that the Hamiltonian of the three-

dimensional q-deformed harmonic oscillator satisfying the above requirements takes the form

$$H_q=\hbar\omega_0\left\{[\mathcal{N}]_q q^{\mathcal{N}+1}-\frac{q(q-q^{-1})}{[2]_q}C_q^{(2)}\right\}, \tag{27}$$

where $\mathcal{N}$ is the number operator and $C_q^{(2)}$ is the second-order Casimir operator of the algebra $\mathrm{so}_q(3)$, while

$$[x]_q=\frac{q^x-q^{-x}}{q-q^{-1}} \tag{28}$$

is the definition of q numbers and q operators.

The energy eigenvalues of the three-dimensional q-deformed harmonic oscillator are then [6]

$$E_q(n,l)=\hbar\omega_0\left\{[n]_q q^{n+1}-\frac{q(q-q^{-1})}{[2]_q}[l]_q[l+1]_q\right\}, \tag{29}$$

where n is the number of vibrational quanta and l is the eigenvalue of the angular momentum, obtaining the values $l=n,n-2,\ldots,0$ or 1.

In the limit of $q\to 1$ one obtains $\lim_{q\to 1}E_q(n,l)=\hbar\omega_0 n$, which coincides with the classical result.

For small values of the deformation parameter τ (where $q=e^{\tau}$) one can expand Eq. (29) in powers of τ obtaining [6]

$$E_q(n,l)=\hbar\omega_0 n-\hbar\omega_0\tau[l(l+1)-n(n+1)]$$
$$-\hbar\omega_0\tau^2[l(l+1)-\tfrac{1}{3}n(n+1)(2n+1)]+O(\tau^3). \tag{30}$$

The number of states characterized by a given value of n, i.e., the number of states in the nth shell, is still given by Eq. (4) if the spin is not taken into account, and by Eq. (6) with spin taken into account.

The total number of particles that can be accommodated in the levels of all shells up to the nth shell included is still given by Eq. (12), with spin taken into account.

The analog of the sum of the eigenvalues of $\mathbf{L}^2$ within each shell in the case of even l is, in analogy with Eq. (7), given by

$$L_{1,q}(n)=\sum_{l=0,l=\text{even}}^{n}[l]_q[l+1]_q(2l+1)$$
$$=\frac{1}{(q-q^{-1})^2(q^2-q^{-2})^2}$$
$$\times\Big((2n+1)(q^{2n+5}+q^{-2n-5})-(2n+5)$$
$$\times(q^{2n+1}+q^{-2n-1})+5(q+q^{-1})-(q^5+q^{-5})$$
$$-\frac{n(n+3)}{2}(q^5+q^{-5}+q^3+q^{-3}-2q-2q^{-1})\Big), \tag{31}$$

where $[l]_q[l+1]_q$ are the eigenvalues of the second-order Casimir operator of $\mathrm{so}_q(3)$, and use of $(2l+1)$ has been made for the degeneracy within a shell without taking spin into account. In performing the relevant summations one needs, in addition to Eq. (5), the sums

$$\sum_{x=0}^{n}e^{\tau x}=\frac{e^{\tau(n+1)}-1}{e^{\tau}-1}, \tag{32}$$

$$\sum_{x=0}^{n}xe^{\tau x}=\frac{1}{(e^{\tau}-1)^2}[ne^{\tau(n+2)}-(n+1)e^{\tau(n+1)}+e^{\tau}], \tag{33}$$

of which the first is a simple geometric series, while the second can be derived from the first through differentiation with respect to the parameter τ. One can easily see that for odd l a result identical to the one given in Eq. (31) is obtained.

Using the definition of the q numbers given in Eq. (28) the above result can be rewritten in the form

$$L_{1,q}(n)=\frac{q^2}{(q^2-1)^2}\Big\{(2n+1)\left[n+\frac{3}{2}\right]_{q^2}-4\left[\frac{n+1}{2}\right]_{q^2}\left[\frac{n}{2}\right]_{q^2}$$
$$-\left(\frac{n}{2}+1\right)(n+1)\left(\left[\frac{3}{2}\right]_{q^2}+\left[\frac{1}{2}\right]_{q^2}\right)+\left[\frac{1}{2}\right]_{q^2}\Big\}, \tag{34}$$

or equivalently,

$$L_{1,q}(n)=\frac{1}{(q-q^{-1})^2}\Big[(2n+1)\frac{[2n+3]_q}{[2]_q}-4\frac{[n]_q}{[2]_q}\frac{[n+1]_q}{[2]_q}$$
$$-\left(\frac{n}{2}+1\right)(n+1)[2]_q+\frac{1}{[2]_q}\Big], \tag{35}$$

where, for example, use of the identity

$$[n]_{q^2}=\frac{q^{2n}-q^{-2n}}{q^2-q^{-2}}=\frac{q^{2n}-q^{-2n}}{q-q^{-1}}\frac{q-q^{-1}}{q^2-q^{-2}}=\frac{[2n]_q}{[2]_q} \tag{36}$$

has been repeatedly made.

Equation (31) can be rewritten in yet another form by using the definition for Q numbers (see, for example, the review article in [3] for relevant details),

$$[n]_Q=\frac{Q^n-1}{Q-1}, \tag{37}$$

where

$$Q=q^2. \tag{38}$$

Using this definition Eq. (31) takes the form

$$L_{1,q}(n)=\frac{Q^3}{(Q-1)(Q^2-1)^2}\{[n]_Q Q^{1/2}[(Q^2-5)+2n\times(Q^2-1)]+[-n]_Q Q^{-1/2}[(Q^{-2}-5)+2n(Q^{-2}-1)]\}-\frac{Q^{1/2}}{2(Q-1)(Q^2-1)}\times[n^2(Q+1)^2-n(Q-1)^2]. \quad (39)$$

In the limit $q\to 1$, keeping terms of order up to τ^2 one can see that Eq. (34) is reduced to Eq. (7), i.e., it is in agreement with the nondeformed case. For this calculation one finds helpful the Taylor expansion of q numbers [3],

$$[n]_q=n\pm\frac{\tau^2}{6}(n-n^3)+\frac{\tau^4}{360}(7n-10n^3+3n^5)\pm\frac{\tau^6}{15120}(31n-49n^3+21n^5-3n^7)+\cdots, \quad (40)$$

where the upper signs correspond to q being a phase factor ($q=e^{i\tau}$ with τ being real), while the lower signs correspond to q being real ($q=e^{\tau}$ with τ being real), as in the present case.

One can now proceed to the calculation of the total energy of the particles up to the nth shell included. Using the identity [3]

$$[n]_q q^{n+1}=Q[n]_Q, \quad (41)$$

where q numbers of Eq. (28) [Q numbers of Eq. (37)] are used in the left- (right-) hand side and $Q=q^2$ [Eq. (38)], one finds that the contribution of the first term of Eq. (29) to the total energy is

$$E_{1,q}(n)=\hbar\omega_0\sum_{x=0}^{n}[x]_q q^{x+1}(x+1)(x+2)=\hbar\omega_0\sum_{x=0}^{n}Q[x]_Q(x+1)(x+2)=\hbar\omega_0\frac{Q}{(Q-1)^4}[(n+1)(n+2)Q^{n+3}-2(n+1)\times(n+3)Q^{n+2}+(n+2)(n+3)Q^{n+1}-2]-\hbar\omega_0\frac{Q}{3(Q-1)}(n+1)(n+2)(n+3), \quad (42)$$

where, in addition to Eqs. (5), (6), (8), (32), and (33) one also needs to use the sum

$$\sum_{x=0}^{n}x^2e^{\tau x}=\frac{1}{(e^{\tau}-1)^3}[n^2e^{\tau(n+3)}-(2n^2+2n-1)e^{\tau(n+2)}+(n+1)^2e^{\tau(n+1)}-e^{2\tau}-e^{\tau}], \quad (43)$$

which is derived from Eq. (33) by differentiation with respect to the parameter τ. Using Eq. (37) one can easily see that Eq. (42) can be put in the more symmetric form

$$E_{1,q}(n)=\hbar\omega_0\frac{Q}{(Q-1)^3}\{(n+1)(n+2)[n+3]_Q-2(n+1)[n+2]_Q(n+3)+[n+1]_Q(n+2)\times(n+3)\}-\hbar\omega_0\frac{Q}{3(Q-1)}(n+1)(n+2)(n+3). \quad (44)$$

In the limit of $Q\to 1$, keeping terms up to T^3 (where $Q=e^T=q^2=e^{2\tau}$ and thus $T=2\tau$) one finds that Eq. (44) agrees with Eq. (13) of the nondeformed case. In this calculation it is helpful to use the Taylor expansion of Q numbers [3],

$$[n]_Q=n+\frac{T}{2}(n^2-n)+\frac{T^2}{12}(2n^3-3n^2+1)+\frac{T^3}{24}(n^4-2n^3+n^2)+\cdots. \quad (45)$$

The contribution of the second term of Eq. (29) to the total energy is found in a similar manner. One has

$$E_{2,q}(n)=-\hbar\omega_0 2\frac{q(q-q^{-1})}{[2]_q}\sum_{x=0}^{n}L_{1,q}(x)=-\hbar\omega_0\frac{2Q}{(Q^2-1)^3}\{Q^4[n]_Q[2(Q^2-1)n+(Q^2-2Q-7)]-Q^2[-n]_Q[2(Q^{-2}-1)N+(Q^{-2}-2Q^{-1}-7)]-\tfrac{1}{6}n^2(n+6)(Q+1)\times(Q^2-1)^2+\tfrac{1}{6}n(Q+1)(Q^4+6Q^3+34Q^2+6Q+1)\}, \quad (46)$$

where Eqs. (5), (8), (31), (32), and (33) have been used and the spin of the particles has been taken into account.

The lower part of the spectrum of the three-dimensional q-deformed harmonic oscillator, calculated from Eq. (29), is shown in Fig. 1(b) as a function of the parameter τ, together with the magic numbers appearing at different parameter values, while in Fig. 1(c) the full spectrum up to about 1500 particles is exhibited. The following comments and comparisons to Nilsson's MO are now in place.

(a) The magic numbers at the left end of both figures are those of the three-dimensional isotropic harmonic oscillator, as in Fig. 1(a).

(b) The magic numbers appearing around $\tau=0.04$ are in agreement with the magic numbers appearing in alkali clusters, up to 1500 (see Ref. [4] for more details), which is the expected limit of validity for theories based on the filling of electronic shells [5], while in the case of Nilsson's MO the agreement is limited to the magic numbers up to 138 [Fig. 1(a)].

(c) Around the parameter value $\tau=0.02$ the magic numbers up to 138 in Fig. 1(b) are a mixture of magic numbers of the three-dimensional isotropic harmonic oscillator and magic numbers appearing around $\tau=0.04$ (magic numbers of alkali clusters). Beyond 138 other magic numbers appear.

(d) Numerical calculations show that in the case of $\tau>0$ the levels within each oscillator shell (characterized by a given value of n) are ordered according to the value of l, with the levels with higher values of l lying lower in energy, because of the last term in Eq. (29). This is indeed the case in Figs. 1(b) and 1(c), although the levels have not been labeled by the quantum numbers n,l because of lack of space. The ordering of the levels within each shell is the same as the one appearing in the case of Nilsson's MO [Fig. 1(a)].

(e) As in Nilsson's MO, the level with $l=n$ lies lowest in energy within each shell. However, in the present case the energy of this level is not decreasing with increasing τ. This is true for all levels of the 3D q-HO: Their energies increase with increasing τ [except in the cases of the levels with $(n,l)=(0,0)$ and (1,1), the energies of which remain constant with increasing τ].

(f) As a consequence of (e), no difficulties related to truncation appear in the present case. Stopping the level scheme at the $l=n$ level of a given shell and taking into account all levels with lower n (i.e., all levels of the shells lying below the given one), one makes sure that all levels up to the given level have been included. Therefore in the 3D q-HO reliable truncations can be made, allowing for the description of systems with many particles. This point is one of the main advantages of the 3D q-HO in comparison to Nilsson's MO.

A few more comments on the comparison between the 3D q-HO and Nilsson's MO are also in order.

(a) The $\langle \mathbf{L}^2 \rangle_n$ term in Nilsson's Hamiltonian [Eq. (1)] has been put in ''by hand'' in order to guarantee that the ''center of mass'' of each shell will remain constant, so that shells will not be compressed because of the presence of the $\mathbf{L}^2$ term. In the case of the 3D q-HO it is clear that the opposite effect is present: The shells are expanded because of the extra terms added by the q deformation. One way to see this is by comparing the first-order corrections appearing in Eq. (30) to the last two terms in Eq. (3). In both cases the $l(l+1)$ term causes compression of the shells, while expansion of the shells is caused by the $n(n+1)$ term in the case of the 3D q-HO and by the $n(n+3)/2$ term in the case of Nilsson's MO. Since the difference of these terms is

$$n(n+1)-\tfrac{1}{2}n(n+3)=\tfrac{1}{2}n(n-1), \tag{47}$$

which is positive for $n>1$, it is clear that the expansion in the case of the 3D q-HO will be stronger than the expansion in the case of Nilsson's MO, which is exactly balanced by the compression caused by the $l(l+1)$ term. As a result, in the case of the 3D q-HO, net expansion of the shells will occur, which will be of first order in the parameter τ. Comparison of Figs. 1(a) and 1(b) clearly shows this effect.

(b) In Nilsson's MO the last two terms in the energy expression of Eq. (3) give no net contribution to the total energy up to the nth shell included, and therefore to the average energy per particle as well, which turns out to be proportional to n [see Eq. (19)]. In the 3D q-HO this dependence of the average energy per particle on n is given by the lowest order contribution from Eq. (44), while the next-order contribution from Eq. (44), as well as the lowest order contribution from Eq. (46), give terms with higher powers of n. This property will have to be taken into account when supershells will be considered.

(c) In both models we have derived exact expressions for the total energy up to the nth shell included, i.e., for systems of particles filling complete shells. In order to consider systems of particles for which the last shell is not full, one has to consider numerical methods, such as the Strutinsky method [11,12], which are beyond the scope of the present study.

IV. SUPERSHELLS IN NILSSON'S MODIFIED OSCILLATOR

For studying the existence and properties of supershells in Nilsson's MO we are going to use the procedure employed by Nishioka *et al.* [2]. For a given number of particles N the single-particle energies $E_j(n,l)$ of the N occupied states are summed up,

$$E(N)=\sum_{j=1}^{N} E_j(n,l). \tag{48}$$

This sum is then divided into two parts: a smooth average part E_{av} and a shell part E_{shell}, which will exhibit the supeshell structure

$$E(N)=E_{av}(N)+E_{shell}(N). \tag{49}$$

For the average part of the total energy a liquid-drop model expansion is used [1]

$$E_{av}(N)=a_1N^{1/3}+a_2N^{2/3}+a_3N. \tag{50}$$

This expansion should be adequate in the case of Nilsson's MO, for which the average energy per particle increases linearly with N [see Eq. (19)], but it should not suffice in the case of the 3D q-HO, for which the average energy per particle contains higher order terms, as we have seen in the preceding section. For the latter case an expansion going up to an N^2 term,

$$E_{av}(N)=a_1N^{1/3}+a_2N^{2/3}+a_3N+a_4N^{4/3}+a_5N^{5/3}+a_6N^2, \tag{51}$$

should be more appropriate. In order to keep the calculations uniform and thus facilitate the comparisons between the two oscillators, we opted for using the expansion of Eq. (51) in all cases, although for Nilsson's MO the first three terms would have been adequate. Therefore in the case of Nilsson's MO very small values will be expected for a_6, the coefficient of the N^2 term.

The results for E_{shell} obtained with Nilsson's MO for eight different values of the parameter μ' (assuming $\hbar\omega=1$) are shown in Fig. 2, while the relevant parameter values

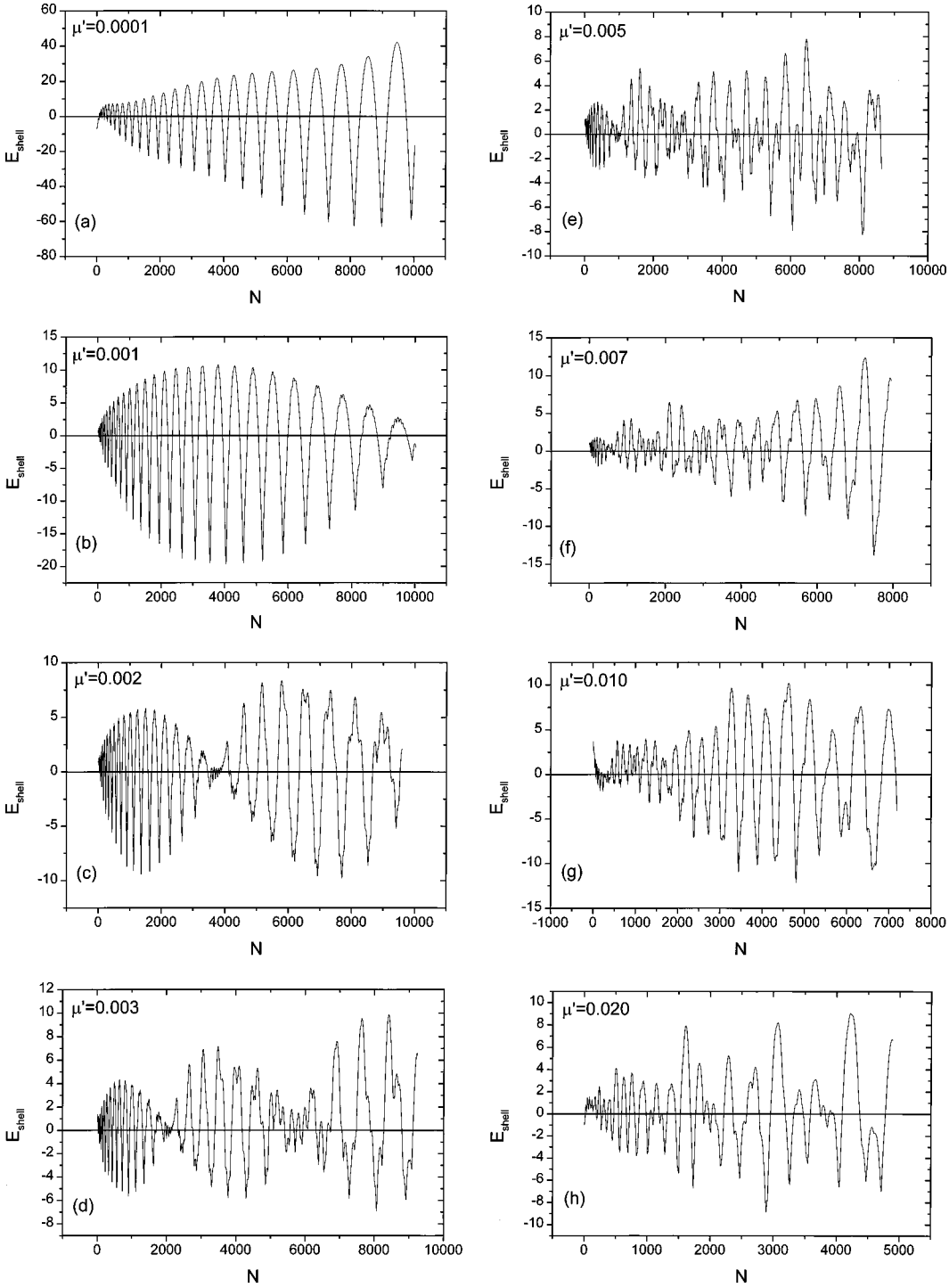

FIG. 2. Shell part (E_{shell}) of the total energy [in units of $\hbar\omega$, see Eq. (3)] for Nilsson's modified oscillator vs the number of particles N. The values of the (dimensionless) parameter μ' are the same as those listed in Table I, together with the details of the calculation. See Sec. IV for further discussion.

and rms deviations are exhibited in Table I. As far as the way of calculation is concerned, the following comments apply:

(a) In all cases the maximum shell used was $n_{max}=30$, implying that the last level included in the calculation was the one with $(n,l)=(30,30)$, in order to ensure that the complete spectrum up to this point has been taken into account, as discussed in Secs. II and III.

(b) From Eq. (26) one sees that for $\mu'=0.02$ one should keep $n<50.5$, while for lower values of μ' the limiting value of n lies even higher. This means that including the shells up to $n=30$ is a reasonable truncation.

(c) The procedure of the calculation was as follows: First the summations described by Eq. (48), resulting in the total energy $E(N)$ for each particle number N, have been performed. Subsequently, in order to reduce the size of the calculation approximately by a factor of 10, the average $E(N)$

TABLE I. Parameters used for fitting the average part of the total energy [see Eq. (51)] in the case of Nilsson's modified oscillator, for various values of the model parameter μ' [see Eq. (3)], corresponding to the cases exhibited in Fig. 2. The parameters are dimensionless, since we have assumed $\hbar\omega=1$ [see Eq. (3)] throughout. The highest shell n_{max} and the number of particles N_{max} included in each calculation, as well as the relevant rms deviation σ, are also shown. See Sec. IV for further discussion.

μ'	a_1	a_2	a_3	a_4	$10^3 a_5$	$10^5 a_6$	n_{max}	N_{Max}	σ
0.0001	13.349	-6.556	−0.218	0.972	4.451	6.853	30	10027	22.06
0.001	−0.025	0.281	−1.482	1.080	0.080	−0.132	30	10027	7.12
0.002	−0.022	0.181	−1.439	1.073	0.489	1.053	30	9609	4.19
0.003	−1.281	1.080	−1.651	1.094	−0.445	0.282	30	9246	3.40
0.005	−1.073	1.013	−1.659	1.096	−0.623	0.043	30	8641	2.76
0.007	−0.830	0.910	−1.654	1.097	−0.724	−0.626	30	7937	4.16
0.01	−5.448	3.432	−2.155	1.143	−2.645	0.383	30	7189	4.88
0.02	5.692	−3.891	−0.376	0.938	9.135	−38.541	30	4890	3.50

was calculated every 11 points (i.e., for $N=6,17,28,\ldots$) up to the point immediately below the cutoff of $(n,l)=(30,30)$, which is reported in Table I as N_{max}. These averaged values of $E(N)$ were subsequently fitted by the expansion of Eq. (51), resulting in the determination of $E_{av}(N)$ at these points. Finally $E_{shell}(N)$ has been obtained at these points as the difference $E(N)-E_{av}(N)$ and plotted in Fig. 2.

On the contents of Table I the following comments can be made.

(a) The behavior of the parameters as a function of μ' is rather smooth, with the exception of a_6, the coefficient of N^2, which assumes very small values, as expected from the comments following Eq. (51).

(b) The maximum number N_{max} of particles below the cutoff is decreasing with increasing μ', as expected from the fact that the level $(n,l)=(30,30)$ is getting lower with increasing μ' [see Eq. (24)].

(c) The rms deviations are very small, given the fact that the relevant average energies range up to 10^6.

On the contents of Fig. 2 the following comments apply.

(a) The gradual development of supershells with increasing μ' is clearly seen in Figs. 2(a)–2(d). While in Fig. 2(a) ($\mu'=0.0001$) no supershell structure is seen up to $N=10\,000$, in Fig. 2(b) ($\mu'=0.001$) the first supershell is seen to be completed around $N=10\,000$, in Fig. 2(c) ($\mu'=0.002$) two supershells are completed up to $N=10\,000$, and in Fig. 2(d) ($\mu'=0.003$) most of the third supershell is also completed by $N=10\,000$.

(b) In Figs. 2(a)–2(g) ($\mu'=0.0001$–0.01) it is clear that N_{s1}, the value of N at which the first supershell is completed, is decreasing as a function of μ'. The same is true for N_{s2}, the value of N at which the second supershell is completed. These trends are not followed by Fig. 2(h) ($\mu'=0.02$). An explanation of this effect can be obtained from Fig. 1(a), in which it is clear that for relatively small μ' ($\mu'<0.01$, for example) the order of the levels remains the same and only their individual energies change, while at $\mu'=0.02$ and beyond, the order of the levels changes drastically, especially at higher energies. This drastic mixing of the levels at $\mu'=0.02$ and beyond can also explain the increasing difficulty in determining the closing of supershells for large μ' especially at high energies, Fig. 2(h) ($\mu'=0.02$) being the clearest example for this case.

(c) According to the study by Balian and Bloch of electrons moving in a spherical cavity [10], which by analogy can be applied to the valence electrons in a metal cluster [1], the minima of the shell energy, E_{shell}, which correspond to shell closures, should appear at equidistant positions (i.e., they should exhibit a periodicity) as a function of $N^{1/3}$ within each supershell. From the data used for plotting Fig. 2 one can see that this condition is approximately fulfilled.

V. SUPERSHELLS IN THE THREE-DIMENSIONAL q-DEFORMED HARMONIC OSCILLATOR

The procedure described in the preceding section has been used in exactly the same way for the determination of supershells in the case of the 3D q-HO.

The results for E_{shell} obtained with the 3D q-HO for ten different values of the parameter τ (assuming $\hbar\omega=1$) are shown in Fig. 3, while the relevant parameter values and rms deviations are exhibited in Table II. In order to facilitate comparisons between the two models, the first eight values of τ used here are the same as the values of μ' used in the preceding section.

As far as the way of calculation is concerned, the maximum shell used in the first eight cases was $n_{max}=30$, as in the preceding section, in order to facilitate comparisons between the two models. Lower n_{max} has been used only in the last two cases, as shown in Table II, in order to keep the rms deviation small.

On the contents of Table II the following comments can be made.

(a) The behavior of the parameters as functions of τ is smooth, even in the case of a_6, the coefficient of N^2, which in the case of Nilsson's MO was not showing smooth behavior.

(b) The maximum number N_{max} of particles below the cutoff is decreasing with increasing τ. This can be explained by looking at Fig. 1(c). The level used as the cutoff is the level with $(n,l)=(n_{max},n_{max})$, which, as explained in Sec. III, is the lowest level within the n_{max}th shell and, as seen in

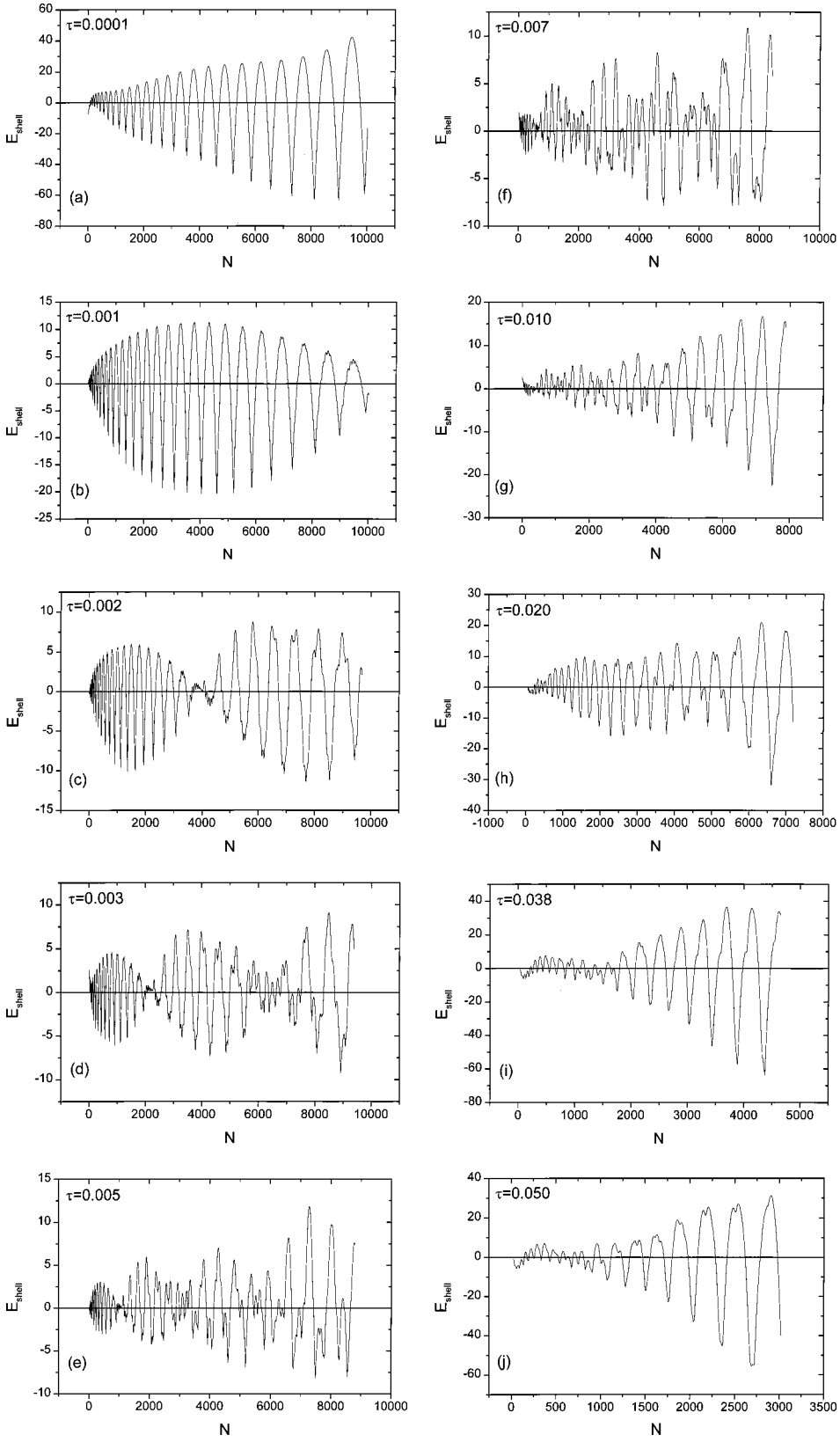

FIG. 3. Shell part (E_{shell}) of the total energy [in units of $\hbar\omega_0$, see Eq. (29)] for the three-dimensional q-deformed harmonic oscillator vs the number of particles N. The values of the (dimensionless) parameter τ are the same as those listed in Table II, together with the details of the calculation. See Sec. V for further discussion.

Fig. 1(c), increases very slowly with increasing τ. It is then clear that the higher the value of τ, the more will be the levels coming from below and crossing over the cutoff level, resulting in the decrease of N_{max} with increasing τ seen in Table II.

(c) As in the case of Nilsson's MO, the rms deviations are very small, given the fact that the relevant average energies range up to 10^6.

On the contents of Fig. 3 the following comments apply.

(a) The gradual development of supershells with increas-

TABLE II. Parameters used for fitting the average part of the total energy [see Eq. (51)] in the case of the three-dimensional q-deformed harmonic oscillator for various values of the model parameter τ [see Eq. (29), with $q=e^{\tau}$], corresponding to the cases exhibited in Fig. 3. The parameters are dimensionless, since we have assumed $\hbar\omega_0=1$ [see Eq. (29)] throughout. The highest shell n_{max} and the number of particles N_{max} included in each calculation, as well as the relevant rms deviation σ, are also shown. See Sec. V for further discussion.

τ	a_1	a_2	a_3	a_4	$10^3 a_5$	$10^5 a_6$	n_{max}	N_{Max}	σ
0.0001	13.585	−6.554	−0.228	0.972	4.464	−6.776	30	10027	22.12
0.001	0.753	−0.061	−1.424	1.073	0.867	−0.272	30	10027	7.58
0.002	1.458	−0.496	−1.318	1.059	2.075	−1.136	30	9686	4.68
0.003	−3.358	2.186	−1.855	1.106	0.615	2.501	30	9389	3.52
0.005	0.667	0.166	−1.500	1.074	2.791	2.422	30	8795	3.49
0.007	−2.631	1.965	−1.867	1.106	2.204	7.580	30	8421	3.88
0.01	−3.657	2.568	−2.013	1.120	2.523	15.399	30	7893	6.75
0.02	−17.409	11.661	−4.267	1.379	−10.052	88.547	30	7189	9.03
0.038	−55.417	41.650	−13.067	2.615	−96.648	482.365	26	4648	17.98
0.05	−64.123	55.364	−19.160	3.777	−202.994	999.866	22	3020	16.63

ing τ is clearly seen in Figs. 3(a)–3(d) ($\tau=0.0001$–0.003), which look very similar to Figs. 2(a)–2(d) ($\mu'=0.0001$–0.003) of the preceding section.

(b) In Figs. 2(a)–2(g) ($\tau=0.0001$–0.01) it is clear that $N_{s1,q}$, the value of N at which the first supershell is completed, is decreasing as a function of τ, almost in the same way as N_{s1} is decreasing as a function of μ' in the case of Nilsson's MO, the only difference being that for numerically equal values of τ and μ' the corresponding value of $N_{s1,q}$ is slightly higher that the relevant value of N_{1s}, a fact that can be explained by the general property of the spectrum of the 3D q-HO to expand more rapidly than the spectrum of Nilsson's MO, as seen in Sec. III. The same is true for $N_{s2,q}$, $N_{s3,q}$, $N_{s4,q}$, i.e., the values of N at which the second, third, and fourth supershells are completed. These trends are not followed by Figs. 3(h) ($\tau=0.02$), 3(i) ($\tau=0.038$), 3(j) ($\tau=0.05$), which correspond to higher values of τ, where the mixing of the levels is very strong in comparison to the picture existing at low values of τ [i.e., for $\tau<0.01$, as seen in Fig. 1(c)].

(c) Despite the fact that the systematics of supershell closures are modified beyond $\tau=0.02$ because of the strong mixing of levels, supershells are still seen beyond this point, while this was not possible in the case of Nilsson's MO, because of truncation-related problems, as we have seen in Sec. III. It should be noticed that this is exactly the region of τ values, which has been found relevant for the description of metal clusters [4].

(d) In the case of alkali clusters, Na, in particular, the first supershell is known to occur around $N=1000$ [2,13–15], which is quite in agreement with what is seen in Fig. 3(i), which corresponds to $\tau=0.038$, the parameter value for which the magic numbers of alkali clusters are correctly reproduced [4] up to 1500 particles, which is the expected limit of validity of theories based on the filling of electronic shells [5]. It should be noticed that only one free parameter exists in the theory, namely, τ, which has been fixed in Ref. [4] in order to reproduce the magic numbers of alkali clusters. Therefore no free parameter has been left over in the calculation of supershells. The fact that the present calculation leads to a reasonable prediction of the position of the first supershell closure is quite a stringent test of the present theory.

(e) As we have already mentioned, the theory by Balian and Bloch [10] for electrons moving in a spherical cavity, which by analogy can be applied to the valence electrons of metal clusters [1], predicts that the minima of the shell energy E_{shell}, which correspond to shell closures, should appear within each supershell at equidistant positions (i.e., they should exhibit a periodicity) when plotted versus $N^{1/3}$. From the data used for plotting Fig. 3 one can see that this condition is approximately fulfilled.

(f) A further prediction of the theory by Balian and Bloch [10] is that the plot of the cubic root $N_i^{1/3}$ of the magic numbers N_i, corresponding to shell closures versus the index i counting the shells, should be a straight line [1]. In the case of alkali clusters, in particular, in which the triangular and squared closed orbits are supposed to dominate [1,13], the slope of the line should be 0.603. In order to make a preliminary estimate of the degree to which this prediction is fulfilled, one can employ the data used in plotting Fig. 3(i), which corresponds to $\tau=0.038$, i.e., to the parameter value found appropriate [4] for reproducing the magic numbers of several alkali clusters. One can then see that this requirement is roughly fulfilled, although the slope appears to be gradually decreasing at large i, an effect that might be due to missing corrections mentioned in comment (h).

(g) In the case of Al clusters, magic numbers have been determined experimentally in detail up to 1200 electrons [16], while additional experimental results up to 2700 electrons exist [17]. The slope of $N_i^{1/3}$ vs i in this case is considerably lower (around 0.32) [1], indicating that closed orbits other than the triangular and squared ones should be present in the Balian and Bloch approach [17]. It will be interesting to examine if the 3D q-HO can provide any prediction for supershells in Al clusters, after choosing the value of the τ parameter in order to reproduce the right slope of $N_i^{1/3}$ vs i.

(h) In order to guarantee the reliability of such predic-

tions, it is of interest to study in advance the influence of any modifications imposed by the Strutinsky method [11,12], which can be applied in cases in which the last shell is open, which are beyond the realm of the present analytic study of Sec. III. The influence of the well-known quantum-mechanical effect that $\hbar\omega_0$ should be decreasing with increasing number of particles in the cluster [8,18,19] should also be taken into account.

VI. DISCUSSION

The main results of the present study are summarized as follows.

(a) The 3D q-deformed harmonic oscillator, which is known [4] to describe very well the magic numbers of alkali-metal clusters up to 1500 particles (the expected limit of validity for theories based on the filling of electronic shells), is found in the present study to be able to produce supershell structures, succesfully predicting the first supershell in alkali clusters without involving any free parameter in addition to the deformation parameter τ, which has been fixed for reproducing the magic numbers.

(b) It should be noticed that these successes of the 3D q-HO are largely due to terms in the Hamiltonian induced by the symmetry, which make the spectrum of the 3D q-HO expand with increasing shell number n more rapidly than the corresponding spectrum of Nilsson's modified oscillator, allowing, among other things, for reliable truncations to be performed.

(c) The successful prediction of the magic numbers can be considered as evidence that the 3D q-deformed harmonic oscillator owns a symmetry [the $u_q(3) \supset so_q(3)$ symmetry, which is a nonlinear deformation of the u(3) symmetry of the spherical (3D isotropic) harmonic oscillator] appropriate for the description of the physical systems under study. The use of this symmetry for predicting supershells in other kinds of metal clusters (Al clusters, for example) is an interesting open problem. The influence of using open shells (taken into account by the Strutinsky method [11,12]), as well as of the well-known quantum-mechanical fact that $\hbar\omega_0$ should be decreasing with increasing number of particles in the cluster [8,18,19], should be taken into account before any final predictions can be made.

ACKNOWLEDGMENT

Support from the Bulgarian Ministry of Science and Education under Contract Nos. Φ-415 and Φ-547 is gratefully acknowledged.

[1] M. Brack, Rev. Mod. Phys. **65**, 677 (1993).
[2] H. Nishioka, K. Hansen, and B. R. Mottelson, Phys. Rev. B **42**, 9377 (1990).
[3] D. Bonatsos and C. Daskaloyannis, Prog. Part. Nucl. Phys. **43**, 537 (1999).
[4] D. Bonatsos, N. Karoussos, D. Lenis, P. P. Raychev, R. P. Roussev, and P. A. Terziev, Phys. Rev. A **62**, 013203 (2000).
[5] T. P. Martin, T. Bergmann, H. Góhlich, and T. Lange, Chem. Phys. Lett. **172**, 209 (1990); Z. Phys. D: At. Mol. Clusters **19**, 25 (1991).
[6] P. P. Raychev, R. P. Roussev, N. Lo Iudice, and P. A. Terziev, J. Phys. G **24**, 1931 (1998).
[7] S. G. Nilsson, Mat. Fys. Medd. K. Dan. Vidensk. Selsk. **29**, 16 (1955).
[8] S. G. Nilsson and I. Ragnarsson, *Shapes and Shells in Nuclear Structure* (Cambridge University Press, Cambridge, 1995).
[9] K. Clemenger, Phys. Rev. B **32**, 1359 (1985).
[10] R. Balian and C. Bloch, Ann. Phys. (N.Y.) **69**, 76 (1972).
[11] V. M. Strutinsky, Nucl. Phys. A **95**, 420 (1967).
[12] V. M. Strutinsky, Nucl. Phys. A **122**, 1 (1968).
[13] C. Bréchignac, Ph. Cahuzac, F. Carlier, M. de Frutos, and J. Ph. Roux, Phys. Rev. B **47**, 2271 (1993).
[14] J. Pedersen, S. Bjørnholm, J. Borggreen, K. Hansen, T. P. Martin, and H. D. Rasmussen, Nature (London) **353**, 733 (1991).
[15] O. Genzken and M. Brack, Phys. Rev. Lett. **67**, 3286 (1991).
[16] J. L. Persson, R. L. Whetten, H. P. Cheng, and R. S. Berry, Chem. Phys. Lett. **186**, 215 (1991).
[17] J. Lermé, M. Pellarin, J. L. Vialle, B. Baguenard, and M. Broyer, Phys. Rev. Lett. **68**, 2818 (1992).
[18] B. A. Kotsos and M. E. Grypeos, in *Atomic and Nuclear Clusters*, edited by G. S. Anagnostatos and W. von Oertzen (Springer, Berlin, 1995), p. 242.
[19] B. A. Kotsos and M. E. Grypeos, Physica B **229**, 173 (1997).